Experimental Evaluation of the Interaction among Neighboring Reinforcements in Geosynthetic-Reinforced Soils

Amr M. Morsy[1]; Jorge G. Zornberg, F.ASCE[2]; Dov Leshchinsky, M.ASCE[3]; Barry R. Christopher, M.ASCE[4]; Jie Han, F.ASCE[5]; and Burak F. Tanyu, M.ASCE[6]

Abstract: This paper presents and interprets experimental results of soil–reinforcement interaction tests conducted using a new device developed to assess the mechanical interaction among neighboring reinforcements in geosynthetic-reinforced soil masses. Testing involved a soil mass reinforced using three reinforcement layers, one of which was actively tensioned while the two neighboring layers remained passive. The neighboring reinforcement layers received stresses from the tensioned reinforcement through the shear stresses transferred to the intermediate soil medium. In this study, a number of soil–reinforcement interaction tests were conducted with different reinforcement and soil types. Test results indicate that the load conveyed to the neighboring reinforcement increased with increasing tension in the loaded reinforcement layer. The magnitude of load transfer was found to increase with increasing soil–reinforcement interaction. At least for the products used in this study, geogrid reinforcements showed a greater ability to form a composite reinforced soil mass than geotextile reinforcements.
DOI: 10.1061/(ASCE)GT.1943-5606.0002365.

Author keywords: Soil reinforcement; Reinforcement interaction; Reinforced soil; Geosynthetics.

Introduction

The interaction between the soil and reinforcement plays a major role in the load transfer between reinforcement and soil in reinforced soil masses. The degree of soil–reinforcement interaction governs the ability of a reinforcement to form a quasi-composite reinforced soil material (i.e., the tendency of reinforcement and soil to behave as a single material under external loads). The spacing between reinforcement layers was reported to control the degree of interaction not only between the reinforcement layer and surrounding soil, but also between neighboring reinforcement layers. This interaction was found to enhance the overall mechanical response of reinforced soil masses (Leshchinsky et al. 1994; Leshchinsky and Vulova 2001; Nicks et al. 2013; Morsy et al. 2017a; Morsy 2017). Reinforcement spacing has been reported to have a greater effect on the stability of a reinforced soil structure than reinforcement tensile strength at ultimate states (Nicks et al. 2013), and greater than the reinforcement tensile stiffness under working stresses (Morsy 2017).

Specifically, Nicks et al. (2013) reported that geosynthetic-reinforced piers of the same ratio of reinforcement tensile strength to reinforcement vertical spacing, T_f/S_v, exhibit different vertical bearing capacities and lateral deformations. The piers reinforced at a comparatively small vertical spacings, less than 0.3 m, showed larger bearing capacity and smaller lateral deformation compared with those reinforced at comparatively larger spacings. Morsy (2017) evaluated a large number of reinforced soil centrifuge models (including slopes and walls). It was concluded that models with the same ratio of reinforcement tensile stiffness to reinforcement vertical spacing, J/S_v, reinforced at different reinforcement spacings failed at different g-levels. Morsy (2017) also reported similar conclusion for centrifuge models with the same and others with the same T_f/S_v and different vertical spacings. A similar conclusion was made by Shen et al. (2019) for two-dimensional (2D) and three-dimensional (3D) finite-difference numerical simulations of the behavior of geosynthetic-reinforced soil piers. The interaction mechanisms that result from the confinement of reinforcements were observed to exhibit behaviors not necessarily consistent with results predicted by limit state analyses (Ziegler 2011). However, the need for a greater understanding of the mechanisms and extent of such an effect remains.

Ketchart and Wu (2002) studied the effect of the interaction between soil and reinforcements in geosynthetic-reinforced soil masses under various loading conditions. The soil and reinforcements were observed to deform interactively under applied vertical loads. Ruiken et al. (2011) conducted large-scale laboratory tests to explore the mechanical behavior of geosynthetic-reinforced systems behaving as composites using an approach similar to that used by Ketchart and Wu (2002). The testing apparatus utilized by Ruiken et al. (2011) was able to identify the effect of displacements on the development and distribution of stresses within the reinforced soil mass. Using the same setup, Jacobs et al. (2013) investigated the load transfer between soil and geogrid based on experimental results. The development of shear zone for various

[1]Assistant Professor, Dept. of Civil Engineering, Cairo Univ., Giza 12613, Egypt (corresponding author). ORCID: https://orcid.org/0000-0002-9335-7847. Email: amr.morsy@eng.cu.edu.eg

[2]Professor, Dept. of Civil, Architectural, and Environmental Engineering, Univ. of Texas at Austin, Austin, TX 78712.

[3]Emeritus Professor, Dept. of Civil and Environmental Engineering, Univ. of Delaware, Newark, DE 19716.

[4]Consultant, Christopher Consultants, 1 Linda Mar Dr., St. Augustine, FL 32080.

[5]Professor, Dept. of Civil, Environmental, and Architectural Engineering, Univ. of Kansas, Lawrence, KS 66045.

[6]Associate Professor, Dept. of Civil, Environmental, and Infrastructure Engineering, George Mason Univ., Fairfax, VA 22030.

Note. This manuscript was submitted on September 24, 2019; approved on May 31, 2020; published online on July 31, 2020. Discussion period open until December 31, 2020; separate discussions must be submitted for individual papers. This paper is part of the ***Journal of Geotechnical and Geoenvironmental Engineering***, © ASCE, ISSN 1090-0241.

reinforced specimens was captured, facilitating the evaluation of different reinforcing mechanisms.

Several factors may affect the thickness of the shear band. A major factor influencing shear band thickness involves soil particle size. Alshibli and Sture (1999) reported that the ratio of shear band thickness to mean particle size decreased with increasing particle size. Bareither et al. (2008) showed that not only does particle size affect the interface friction, but particle roundness also contributes to the soil–geosynthetic interface behavior. Therefore, the thickness of the shear band is expected to vary significantly for granular soil particles. Fannin and Raju (1993) showed that textured geomembranes mobilize thicker shear bands than smooth geomembranes. Soil arching may also take place in reinforced soil, especially in cases involving closely spaced reinforcements where shear bands of neighboring soil–reinforcement interfaces are expected overlap. This phenomenon is expected to depend on the soil density, grain size, normal stress, and interface characteristics (Leshchinsky et al. 1994; Morsy et al. 2017a, b, 2018, 2019b).

A new soil–geosynthetic interaction device was developed as part of this study, which could successfully measure the displacement along the length of one reinforcement layer loaded in tension, soil–reinforcement interface relative displacement along the loaded reinforcement layer, displacements in the soil field near the loaded reinforcement layers, and the displacement along the length of two neighboring reinforcement layers placed at a given vertical spacing of the loaded reinforcement layer (Morsy 2017; Morsy et al. 2019a). This paper evaluates the effect of reinforcement and fill material properties on the soil–reinforcement interaction and on the interaction among neighboring reinforcement layers through a testing program conducted using the new soil–geosynthetic interaction device.

The testing program was designed to evaluate the effects of the following aspects on soil–reinforcement interaction: (1) reinforcement tensile stiffness; (2) reinforcement type (grids versus textiles); (3) geogrid reinforcement rigidity (extruded versus knitted grids); and (4) soil type (gravel versus sand). The paper provides a parametric evaluation considering these aspects. The study presented herein corresponds to the experimental component of a comprehensive evaluation of the effect of vertical spacing on the design of geosynthetic-reinforced soil structures (Morsy 2017; Zornberg et al. 2018).

Experimental Approach

A new soil–reinforcement interaction experimental device, shown in Fig. 1, was designed and developed by Morsy (2017) to evaluate

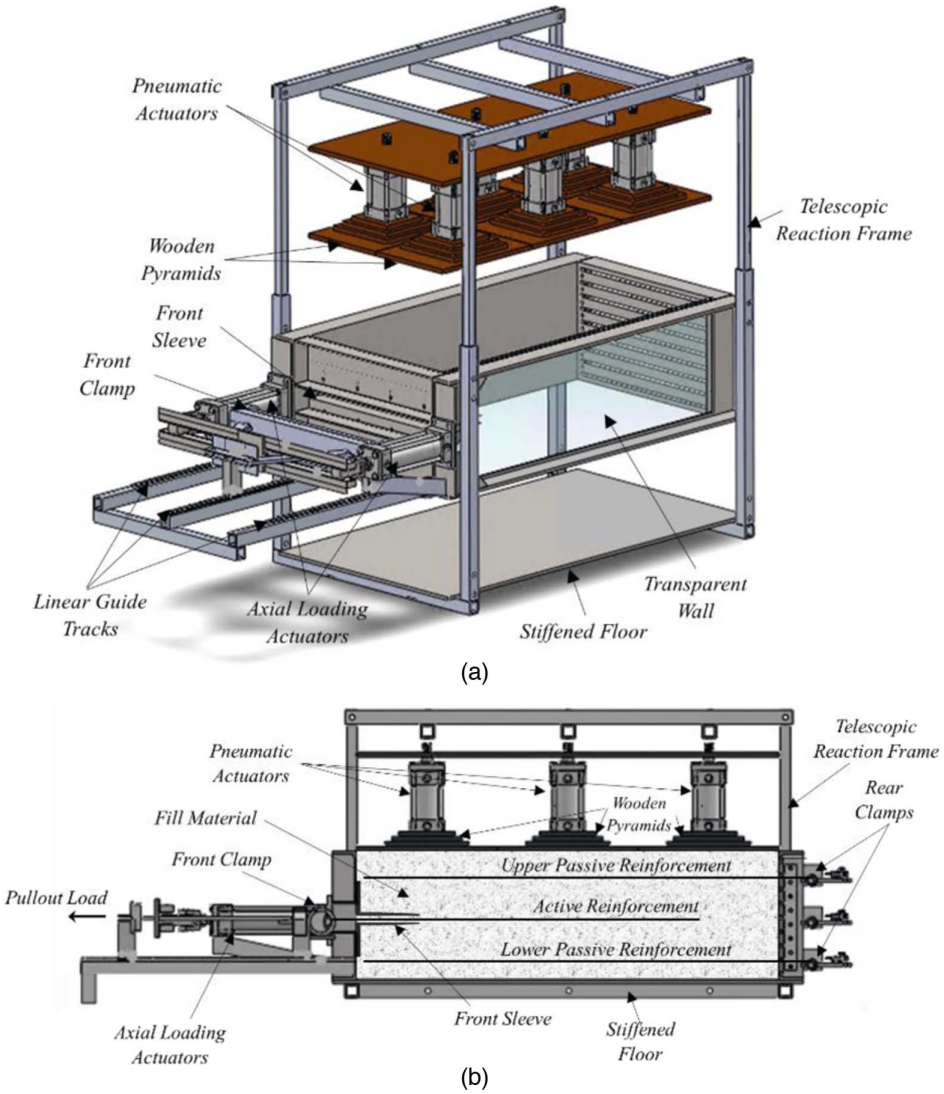

Fig. 1. Soil–geosynthetic interaction device: (a) general layout; and (b) schematic cross section.

J. Geotech. Geoenviron. Eng., 2020, 146(10): 04020107

soil–reinforcement interaction and quantify the thickness of the soil shear band that develops around the soil–reinforcement interface as interface shear stresses are generated. The device accommodates reinforced soil specimens with dimensions up to 1,200 mm deep, 150 mm long, and 750 mm wide. Normal stresses are applied using six pneumatic actuators placed on distributing wooden pyramids that cover the reinforced soil mass, which was found to effectively apply uniform normal stress on top of the reinforced soil mass (Morsy et al. 2019a). Tensile loads are applied to reinforcement layers using an axial loading system consists of two hydraulic actuators. The axial loading system applies tension to the active reinforcement through a clamping system to which the reinforcement is affixed.

The embedded reinforcement layer was subjected to increasing loads, with focus on the response under loads representative of working stress and ultimate tensile stress conditions. In addition to the active reinforcement layer, on which the load is applied, two additional passive reinforcement layers of the same type are used to represent neighboring reinforcements. This signifies relative deformation of neighboring reinforcement layers. Such relative movement exists in a deformable reinforced soil system such as reinforced soil walls where reinforcements at different elevations strain differently. The hypothesis is that this relative movement results in load transfer (or load shedding) among neighboring layers, thus making the multilayer reinforced soil system more efficient exhibiting compositelike behavior (Leshchinsky et al. 1994; Leshchinsky and Vulova 2001; Morsy 2017; Morsy et al. 2019b; Zornberg et al. 2018, 2019). The testing device used in this study was developed to study potential load transfer among adjacent layers occurring when these layers deform differently.

The device was instrumented to monitor the potential interaction occurring between neighboring reinforcement layers. The instrumentation used in the soil–geosynthetic interaction device included (1) a load cell to measure the tensile load applied to the active reinforcement, (2) load cells at the pneumatic actuators to monitor the actual normal pressure applied on top of the reinforced soil mass, (3) sensors to measure displacements at multiple locations within the active and passive reinforcements (shown in Fig. 2 as u1 through u10 for the active reinforcement, v1 through v5 for the upper passive reinforcement, and w1 through w5 for the lower passive reinforcement), and (4) artifical gravel particles buried within the soil mass (shown in Fig. 3 as x1 through x7) and connected to displacement sensors via horizontal telltales to measure internal soil displacements. Detailed descriptions of the testing equipment and the instrumentation and monitoring techniques have been presented by Morsy (2017) and Morsy et al. (2019a). Capabilities and limitations of the testing equipment were also presented by Morsy et al. (2019a).

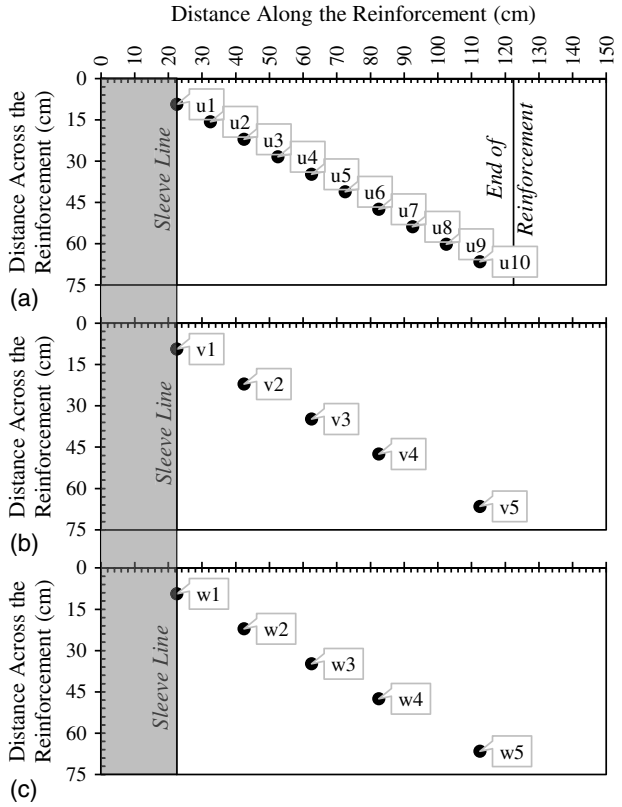

Fig. 2. Plan view of the testing model showing locations of telltale connections: (a) active reinforcement; (b) upper passive reinforcement; and (c) lower passive reinforcement.

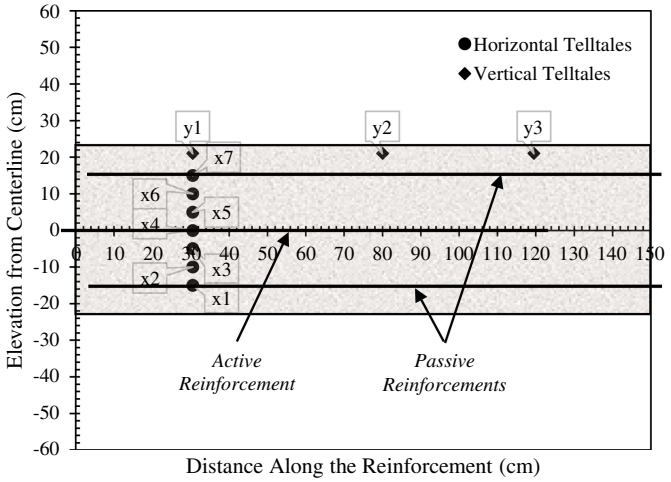

Fig. 3. Vertical cross section of the testing model showing locations of artificial gravel particles within the reinforced soil mass.

Testing Program

The equipment was used in a 450-mm-tall configuration, with dimensions of 1,500 × 300 × 450 mm (length × width × height). Three reinforcement layers were placed at a vertical spacing, S_v, of 0.15 m. The target normal pressure at the middle (active) reinforcement layer was 21 kPa. This normal pressure was intended to be comparatively low to allow pullout failure to occur before reinforcement rupture, which facilitated investigating the soil–reinforcement interaction over a wider range of deformation up (or close) to pullout failure. This approach allowed a more comprehensive understanding of the soil–reinforcement load-transfer mechanisms and an assessment of the soil–reinforcement interaction behavior. The embedment length of the main reinforcement layer was 1,016 mm, and the neighboring (passive) reinforcement layers were extended to the rear of the reinforced soil mass, where they were clamped.

To assess the effect of reinforcement properties (type, tensile stiffness, soil–reinforcement interaction, and ultimate strength) on the interaction between neighboring reinforcement layers in geosynthetic-reinforced soil structures, the program included tests conducted under the same conditions using different reinforcement and soil types. Table 1 summarizes the tests carried out in this study.

Table 1. Summary of tests

Test ID	Testing variables					
	Fill material	S_v	σ_v	Active geosynthetic	Passive geosynthetic	Dilation
GP-06-03-G1-G	Gravel	0.15 m	21 kPa	W1-GT	W1-GT	Allowed
GP-06-03-G2-G	Gravel			W2-GT	W2-GT	
GP-06-03-G4-G	Gravel			EX-GG	EX-GG	
GP-06-03-G5-G	Gravel			KN-GG	KN-GG	
SP-06-03-G1-G	Sand			W1-GT	W1-GT	

Table 2. Characteristics of soils used in soil–geosynthetic interaction tests

Properties	Gravel	Sand
Gradation	Poorly graded	Poorly graded
Particle size range, $\boldsymbol{D}$ (mm)	1.0–13.0	0.2–2.0
Mean particle size, $\boldsymbol{D}_{50}$ (mm)	7.0	0.7
Uniformity coefficient, $\boldsymbol{C}_u$	1.6	1.9
Curvature coefficient, $\boldsymbol{C}_c$	0.9	1.3
Specific gravity, $\boldsymbol{G}_s$	2.62	2.65
Range of void ratio, $\boldsymbol{e}_{\min}$–$\boldsymbol{e}_{\max}$	0.50–0.73	0.56–0.76
AASHTO classification	A-1-a	A-3
USCS classification	GP	SP
Particle roundness	Subrounded to subangular	Rounded to subrounded

Note: AASHTO= American Association of State Highway and Transportation Officials; and USCS = Unified Soil Classification System.

Five tests were conducted using gravel and sand fills and three reinforcement layers placed at a vertical spacing of 0.15 m. The normal stress at the active reinforcement layer was 21 kPa for all tests. The loading rate was set at approximately 0.1 mm/min at the front of the embedded reinforcement zone (i.e., the rate of change in u1 was approximately 0.1 mm/min).

Fill Materials

One baseline fill material was used in most of the tests conducted in this study. The selected material was a clean gravel that could be used in an air-dried condition. An additional granular material (a sand) was also selected to evaluate the effect of grain size. The two materials used in the testing program are described as follows.

Gravel

The baseline fill material used in most of the tests was a washed river pea gravel deposited by the Colorado River near Austin, Texas. The characteristics of this material are summarized in Table 2. The fill was placed in 75-mm-thick lifts and gently hand tamped until a relative density of 70% was reached, which corresponds to a dry unit weight of 16.67 kN/m^3 and a void ratio of 0.57. The shear strength of the fill used in this study was evaluated via a set of isotropic consolidated drained triaxial tests conducted at three different confining stress levels of 35, 70, and 105 kPa and a relative density of 70%. The peak friction angle was 36.9° with y-intercept of 15.6 kPa for the range of confining stresses at which the specimens were tested.

Sand

Monterey Sand No. 30 was used in one soil–geosynthetic interaction test for the purposes of comparison to evaluate the effect of grain size on the soil–reinforcement interaction behavior. This sand was procured from a quarry near Monterey, California. The characteristics of this material are summarized in Table 2. The sand was placed in 75-mm-thick lifts at a moisture content of 3.5% and compacted to a relative density of 70%, which corresponds to a dry unit weight of 16.05 kN/m^3 and a void ratio of 0.62. Samples were taken from every lift during compaction and during soil removal after completion of testing to confirm the homogeneity of the moisture content within the reinforced soil mass. The shear strength of this sand was evaluated via a set of isotropic consolidated drained triaxial tests reported by Zornberg (2002), where the peak friction angle at a relative density of 70% was estimated as 36.7°.

Reinforcement Materials

Four geosynthetic reinforcement types were used in the soil–reinforcement interaction tests conducted as part of this study: (1) W1-GT (Mirafi HP570 of TenCate, Nijverdal, Netherlands) woven polypropylene geotextile; (2) W2-GT (Mirafi RS580i of TenCate, Nijverdal, Netherlands) woven polypropylene geotextile; (3) EX-GG (BX1200 of Tensar, Atlanta, Georgia) extruded (rigid) polypropylene biaxial geogrid; and (4) KN-GG (Fortrac 80T of Huesker, Gescher, Germany) knitted (flexible) polyester uniaxial geogrid. The mechanical properties of the reinforcement materials in the direction where they were tested in the soil–geosynthetic interaction device are summarized in Table 3. The reinforcement tensile stiffness values were not used in data processing and are only reported for possible future use of the presented data. Specimen-specific tensile behavior data were obtained during the soil–geosynthetic interaction test as presented by Morsy et al. (2019a).

Table 3. Characteristics of reinforcements used in this study

Mechanical properties	W1-GT (XMD[a])	W2-GT (XMD[a])	EX-GG (XMD[a])	KN-GG (MD[b])
Ultimate tensile strength, $\boldsymbol{T}_{\text{ult}}$ (kN/m)	70.0	70.0	28.8	89.6
Tensile strength at 5% axial strain, $\boldsymbol{T}_{@5\%}$ (kN/m)	43.8	70.0	19.6	45.7
Secant tensile stiffness at 5% axial strain, $\boldsymbol{J}$ (kN/m)	876	1,400	392	914
Type	Woven geotextile	Woven geotextile	Extruded biaxial geogrid	Knitted uniaxial geogrid
Material	Polypropylene	Polypropylene	Polypropylene	Polyester

[a]XMD = cross-machine direction (cross-rollway direction).
[b]MD = machine direction (rollway direction).

Test Results and Parametric Evaluation

Comparisons were made among the results obtained as part of the experimental testing program in order to evaluate various soil-reinforcement properties: (1) reinforcement tensile stiffness; (2) geosynthetic type (geotextile versus geogrid); (3) reinforcement rigidity (extruded versus knitted geogrids); and (4) soil type (gravel versus sand). These soil-reinforcement properties are evaluated regarding their effect on four different aspects of the soil–reinforcement behavior: (1) effect on frontal tensile load-displacement curves determined at the front of the confined reinforcement zone (i.e., at the interior edge of the sleeve); (2) effect on the thickness of the zone of soil–reinforcement interaction; (3) effect on the relative displacement between soil and reinforcement; and (4) effect on the interaction between neighboring reinforcement layers. More specifically, the soil-reinforcement properties identified for parametric evaluation were organized by conducting the following specific comparisons:

- A comparison between tests conducted with W1-GT and W2-GT geotextile reinforcements to evaluate the effect of reinforcement tensile stiffness on soil–reinforcement interaction. Both reinforcements are woven geotextiles made of the same material (polypropylene) and produced by the same manufacturer. In addition, both reinforcements have the same ultimate tensile strength 70 kN/m. The major differences between both materials are the tensile stiffness and fabric integrity (integrity of longitudinal and transversal yarns). The unconfined tensile stiffness values for W1-GT and W2-GT are 876 and 1,400 kN/m at 5% tensile strain, respectively. W2-GT has more rigid fabric and its longitudinal and transversal yarns are more integrated (yarns are more difficult to separate) than W1-GT. Gravel fill was used in both tests.
- A comparison between tests conducted with W1-GT geotextile and KN-GG geogrid reinforcements to evaluate the effect of geosynthetic type (textile versus grid) on soil–reinforcement interaction. Both reinforcements have similar tensile stiffnesses: the tensile stiffnesses for W1-GT and KN-GG are 876 and 914 kN/m at 5% tensile strain, respectively. Gravel fill was used in both tests.
- A comparison between tests conducted with EX-GG and KN-GG geogrid reinforcements to evaluate the effect of reinforcement rigidity (i.e., the ability to accommodate out-of-plane deformation during fill placement) on soil–reinforcement interaction. The tensile stiffnesses of these reinforcements are reasonably different: the tensile stiffnesses for EX-GG and KN-GG are 392 and 914 kN/m at 5% tensile strain, respectively. Gravel fill was used in both tests.
- A comparison between tests conducted with gravel and sand fills to evaluate the effect of soil type (gravel versus sand). Both soils are uniformly graded, but differ greatly in particle size, and are classified as GP and SP according to the Unified Soil Classification System (USCS), respectively. The gravel and sand have angles of internal resistance of 36.9° and 36.7° at 70% relative density, respectively. This comparison can provide information about the effect of particle size on soil deformation patterns around a loaded reinforcement layer. W1-GT geotextiles were used in both tests.

Effect on Frontal Tensile Load-Displacement Curves

An evaluation was conducted for the impact of the soil–reinforcement properties affecting the frontal tensile load-displacement curves, which includes their effect on the reinforcement tensile stiffness (relevant under working stress conditions) and ultimate pullout resistance (relevant under failure conditions). Fig. 4 shows the frontal pullout load-displacement curves obtained for tests involved in the four comparisons made in this study. Specifically, Figs. 4(a–d) present comparisons of frontal tensile load-displacement curves for test pairs to evaluate the effect of axial tensile stiffness, geosynthetic type, geosynthetic rigidity, and fill type, respectively.

The soil–reinforcement interaction coefficient, C_i, at ultimate frontal tensile load was used as an indicator for soil–reinforcement interaction. This coefficient is usually referred to the efficiency factor and is defined as the ratio of the tangent of equivalent soil–reinforcement angle of interface friction, δ, to the tangent of soil angle of internal friction, φ. This factor was used in this study to provide a basis for comparison between tests conducted with different fill and reinforcement materials under the same testing conditions. The choice of C_i was based on three reasons: (1) it has been widely used in soil-reinforcement practice; (2) it does not require additional testing to obtain; and (3) it is insensitive to the parameters varied in the tests conducted in this study. Soil–reinforcement interaction coefficient C_i can be written as follows:

$$C_i = \frac{T_{\text{ult}}}{2L\sigma_v' \tan\varphi} \tag{1}$$

where T_{ult} = ultimate frontal tensile load reached when the end of the active reinforcement displaces at the same rate of the reinforcement front; L = reinforcement length embedded in the fill; σ_v' = vertical normal stress at the active reinforcement layer elevation; and φ = friction angle of the fill. Table 4 summarizes the soil–reinforcement interaction coefficients for the tests conducted in this study (various combinations of reinforcements and soil types).

Fig. 4(a) shows that the frontal load-displacement curves for the tests conducted using W1-GT and W2-GT reinforcements with gravel coincided up to a frontal displacement of 10 mm. However, beyond 10 mm, W2-GT exhibited lower unit tension. This comparison highlights the relevance of the soil–reinforcement interface shear behavior for both reinforcements used with the gravel in testing. Although the slope of the frontal tensile load-displacement may be very similar for both reinforcements, the ultimate tensile load, and in turn C_i, were greater for W1-GT as compared with W2-GT. This is attributed to the integrity of the fabric (integrity of longitudinal and transverse yarns), which plays a significant role in the interaction between fabric and the surrounding soil medium by adding resistance to the interface friction. Forensic investigation of the exhumed reinforcement layers after testing was completed revealed the presence of intruding holes in W1-GT caused by the adjacent gravel particles. This type of interaction mobilizes passive resistance interaction mechanisms similar to those developed by transverse ribs in geogrid reinforcements. In contrast, such holes were not visible in W2-GT due to its high fabric integrity.

Fig. 4(b) shows the frontal load-displacement curves for the tests conducted with W1-GT and KN-GG reinforcements with gravel. The results indicate that the resistance to pullout for KN-GG was higher than that for W1-GT, with the difference in unit tension increasing as testing progressed. The soil–reinforcement interaction in this case involves two components: (1) the passive resistance mobilized by the transverse members, which can be transverse ribs in geogrids or transverse yarns in geotextiles if particles are able to interfere with the geotextile fabric as previously discussed; and (2) the interface friction. The soil–reinforcement interaction (represented by C_i) was observed to be higher in KN-GG than in W1-GT (Table 4). Although KN-GG is a uniaxial geogrid with comparatively weak junctions (knitted longitudinal and transverse ribs), the contribution of passive resistance to the soil–reinforcement interaction was considerable. Forensic investigation

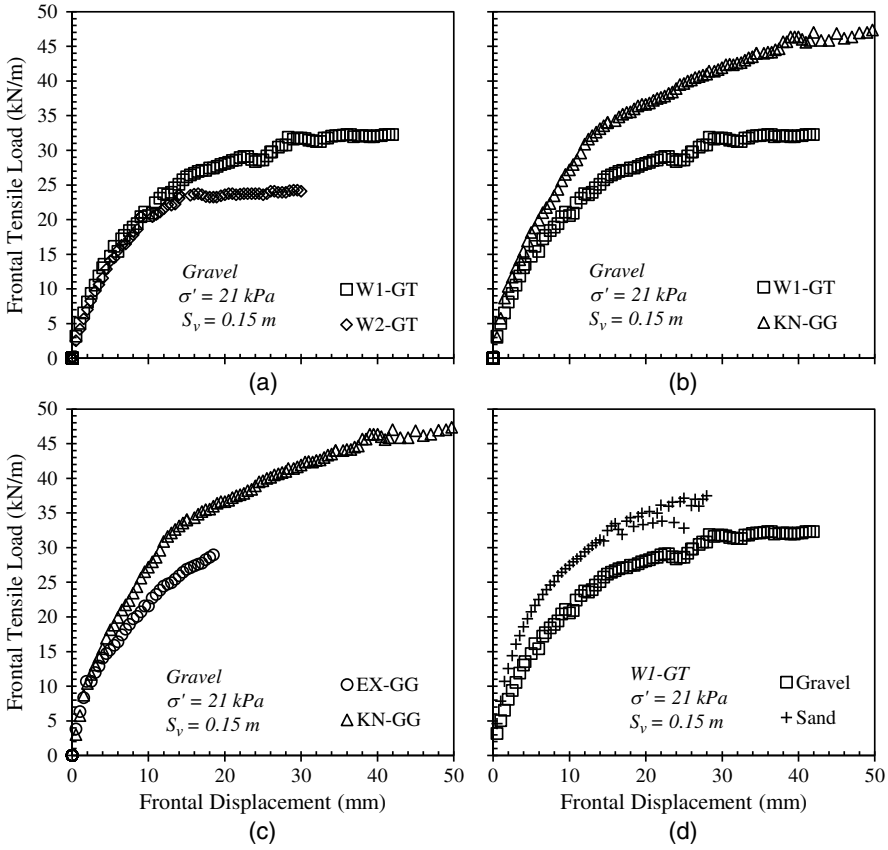

Fig. 4. Frontal tensile load-displacement curves: (a) effect of axial tensile stiffness; (b) effect of geosynthetic type; (c) effect of geosynthetic rigidity; and (d) effect of fill type.

Table 4. Soil–reinforcement interaction coefficients

Soil/reinforcement combination	C_i
W1-GT/gravel	1.0
W2-GT/gravel	0.7
EX-GG/gravel	1.2[a]
KN-GG/gravel	1.5
W1-GT/sand	1.1

[a]An extrapolated value of ultimate tensile loading was used.

of the reinforcement after testing revealed good integrity of the longitudinal and transverse ribs. The passive resistance of KN-GG was found to outweigh the interface friction and passive resistance of W1-GT associated with the interlocking caused by intruding soil particles.

Fig. 4(c) shows the frontal load-displacement curves for the tests conducted with EX-GG and KN-GG geogrids with gravel. The results indicate that KN-GG had a higher resistance to pullout than EX-GG, with the difference in unit tension increasing as testing progressed. However, unlike KN-GG, EX-GG failed in rupture before undergoing considerable soil–reinforcement interface displacement due to its comparatively low tensile strength and stiffness. In this case, the comparison between the frontal load-displacement curves does not provide a full understanding of the soil–reinforcement interaction between the two reinforcements because the tensile stiffness is quite different for each reinforcement. However, the frontal load-displacement curve of EX-GG was extrapolated to determine approximate value for C_i which is essential for comparison. The extrapolated ultimate frontal tensile load for EX-GG was much lower than that of KN-GG. Whereas C_i for EX-GG was obtained using an extrapolated value of ultimate frontal tensile load, the comparisons made in the paper were based on the measured displacement data only, which are representative of the working stresses for such reinforcement. The extrapolated ultimate frontal tensile load was obtained for EX-GG only for further comparison based on C_i.

Fig. 4(d) shows the frontal load-displacement curves for the tests conducted with gravel and sand with W1-GT geotextile reinforcements. The results indicate that the resistance to reinforcement tension obtained for the test conducted using sand was higher than that obtained for the test conducted using gravel under both working stress and ultimate stress conditions. This observation revealed that the soil–reinforcement interaction (represented by C_i) was higher between W1-GT and sand than that between W1-GT and gravel. This was attributed to the larger number of contacts the sand (small particle size) has with a geotextile per unit area compared with gravel (large particle size), which results in more interlocking points. Both soils have similar angles of internal friction.

The interaction between woven geotextiles and soils depends on a number of aspects that can be related to the geotextile and fill material types. These aspects can be summarized as follows:

- Roughness of the geotextile surface, which increases the friction between geotextiles and soils.
- Fabric integrity (integrity of longitudinal and transversal yarns), which control the ability of the soil particles to intrude into geotextiles mobilizing passive resistance with the transverse yarns.
- Size of soil particles with respect to the size of reinforcement weave interval (center-to-center distance between two successive yarns), which control the interlocking between the soil particles and yarns (acting as surface ridges) of geotextiles, even

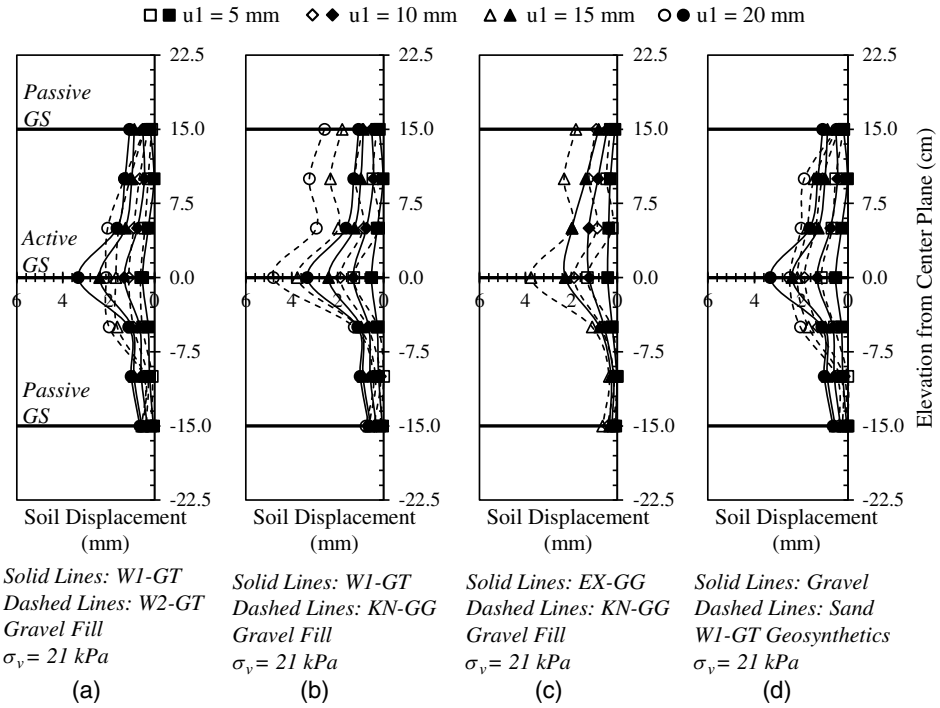

Fig. 5. Horizontal soil displacement profiles at times corresponding to the same frontal displacement u1: (a) effect of axial tensile stiffness; (b) effect of geosynthetic type; (c) effect of geosynthetic rigidity; and (d) effect of fill type.

without particles intrusion. In addition, a smaller soil particle size allows a larger number of particles per unit area to interlock with the geotextile.

- Soil particles' shape and roughness, which controls the ability of the soil to intrude into geotextiles and/or to interlock with the geotextile yarns.

Overall, based on the tests conducted in this study, the results indicated that geotextile reinforcements with ability to soil particle intrusion, due to low fabric integrity, are capable of developing passive resistance, which enhances the soil–reinforcement interaction (i.e., provides higher C_i). Geogrid reinforcements are more capable of interacting with soils than geotextiles. Flexible (knitted) geogrids have higher ability to interact with soil particles than rigid (extruded) geogrids. Sand fills (small particle size) can provide a larger number of contacts (interlocking points) with a geotextile per unit area than gravel fills (large particle size) of similar friction angles.

Effect on the Thickness of the Zone of Soil–Reinforcement Interaction

Fig. 5 presents the horizontal soil displacement profiles measured at the time that the active reinforcement reached specific values of frontal displacement, u1 [Fig. 2(a) shows the location corresponding to u1]. Specifically, the profiles were defined at the time that the displacement at the loading front u1 reached values of 5, 10, 15, and 20 mm, as obtained for the tests involved in the four soil reinforcement variables being considered in this parametric evaluation. Specifically, Figs. 5(a–d) present comparisons of horizontal soil displacement profiles for test pairs to evaluate the effect of axial tensile stiffness, geosynthetic type, geosynthetic rigidity, and fill type, respectively. These profiles, located 80 mm from the sleeve line (i.e., 305 mm from the front wall), involve horizontal displacements measured at specific elevations by tracking artificial gravel particles placed in a vertical array (Fig. 3).The profiles presented in the figure were defined at the same distance from the point of load application (i.e., 80 mm from the sleeve line) and same elevations.

Fig. 5(a) shows the horizontal soil displacement profiles for the tests conducted with W1-GT and W2-GT reinforcements using gravel fill (with W2-GT being approximately twice as stiff as W1-GT). The results indicate that the soil displacements for W1-GT and W2-GT reinforcements in early loading stages were very similar, up to u1 of 10 mm, at which point a difference in the soil–reinforcement interaction was observed that was primarily attributed to the additional passive resistance W1-GT mobilized as discussed previously. Thereafter, soil displacements measured for W1-GT were higher than those measured for W2-GT. It was also observed that the soil adjacent to the reinforcement exhibited a higher displacement gradient than soil father away from the reinforcement because the transferred shear stress (and shear strain) in the fill material decreases with the distance from the reinforcement, resulting in earlier yielding in the internal shear strength of the fill material near the reinforcement. This yielding limits the load transfer from the reinforcement to distances farther away from the reinforcement.

Fig. 5(b) shows the horizontal soil displacement profiles for the tests conducted with W1-GT and KN-GG reinforcements also using gravel as fill material. The results indicate smaller soil displacements for W1-GT as compared with KN-GG. This difference was observed to increase as loading progressed due to the difference the soil–reinforcement interaction (represented by C_i) between the two reinforcement types. Also in this case, the soil adjacent to the reinforcement exhibited higher displacement gradients than at more distant locations from the reinforcement. This is consistent with yielding that occurs after reaching the internal shear strength of the fill material near the soil reinforcement interface, which limits the load transfer from the reinforcement to distances farther away from the reinforcement.

Fig. 5(c) shows the horizontal soil displacement profiles for the tests conducted with EX-GG and KN-GG geogrids using

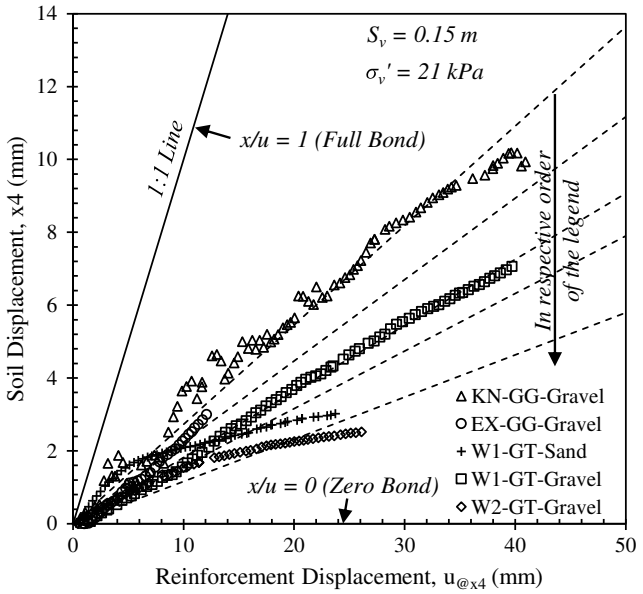

Fig. 6. Relationship of active reinforcement displacements and adjacent soil displacements.

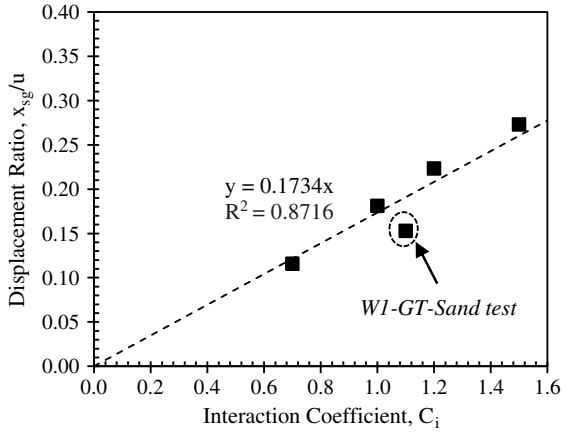

Fig. 7. Soil–reinforcement interaction coefficient, C_i, versus displacement ratio, x_{sg}/u.

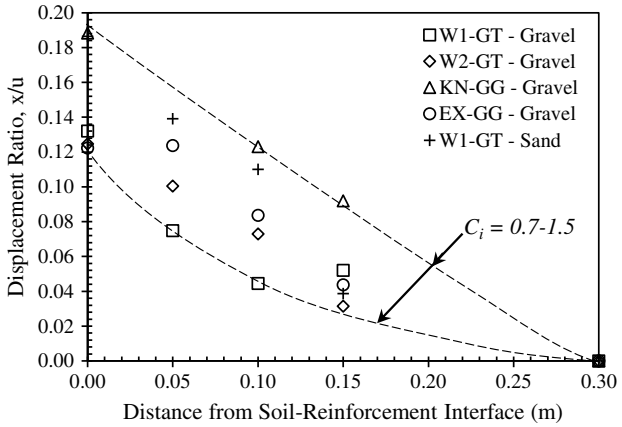

Fig. 8. Soil to reinforcement displacement ratio at various distances from active reinforcement.

gravel fill. The results indicate smaller soil displacements for EX-GG as compared with KN-GG. This difference increased as loading progressed due to the difference in soil–reinforcement interaction (represented by C_i) between the two reinforcement types.

Fig. 5(d) shows the horizontal soil displacement profiles for the tests conducted with gravel and sand, using W1-GT geotextiles in both cases. The results indicate that the soil displacements measured in sand were higher than those measured in gravel at early loading states and lower at later stages. This indicates that soil–reinforcement interface shear resistance yields at a lower stress in case of sand as compared with the case of gravel. In addition, the soil adjacent to the reinforcement exhibited a higher displacement gradient for the gravel than for the sand.

Fig. 6 presents the relationship between the horizontal soil displacements adjacent to the reinforcement measured using the artificial gravel particle x4 (Fig. 3) and the reinforcement displacements at the same location obtained by interpolation between measured displacements u1 and u2 [Fig. 2(a)]. The relationship was found to be fairly linear for the various tests conducted in this study with exception to the test conducted with sand fill, which showed slightly nonlinear relationship. The slope of the linear relationship (i.e., soil to reinforcement displacement ratio) was found to increase with increasing the soil–reinforcement interaction (represented by C_i).

Fig. 7 shows the relationship between C_i and the soil to reinforcement displacement ratio. The relationship was found to be linear and can be written in the following form:

$$C_i = 0.17\frac{x_{sg}}{u} \tag{2}$$

where x_{sg} = horizontal soil displacement at the soil–reinforcement interface; and u = reinforcement displacement at the location corresponding to x_{sg}. Although the data presented in this paper were obtained for only five tests, Eq. (2) satisfies data obtained from a total of 19 tests presented by Morsy (2017), Zornberg et al. (2018), and Morsy et al. (2019b). Overall, the soil–reinforcement interaction (represented by C_i) controls the deformation of the soil mass adjacent to a loaded reinforcement layer. As C_i increases, the synergy between the soil and reinforcement in a reinforced soil mass increases.

Soil displacement patterns can be used to predict the extent of the interaction between reinforcement layers and soils. The ratio of soil to reinforcement displacement (x/u) was used as an indicator of the interaction between reinforcement layers and soil layers. Fig. 8 shows the soil to reinforcement displacement ratio as a function of the distance away from the active reinforcement. The influence of reinforcement and fill types on the soil to displacement ratio was inferred from the tests involved in the four comparisons made in this study. The figure presents envelopes that were plotted at the boundaries of the data generated in the tests conducted in this study. The envelopes were drawn to approach the x-axis at a distance of approximately 0.30 m, which is the upper boundary for the zone of soil–reinforcement interaction identified by Morsy (2017), Zornberg et al. (2018), and Morsy et al. (2019b). The presented results suggest that the interaction between reinforcement and soil layers decreases exponentially with the distance from the soil–reinforcement interface. The degree of interaction increases with increasing the soil–reinforcement interaction (represented by C_i). Such interaction allows the reinforced soil mass to form a composite mass.

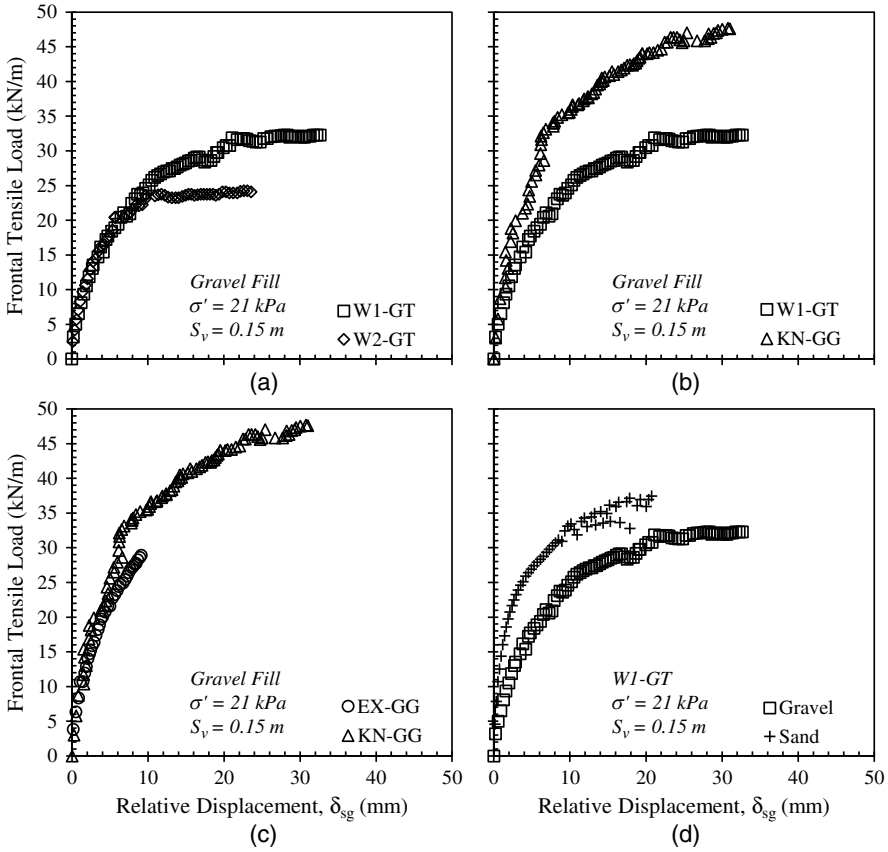

Fig. 9. Relative displacement between soil and reinforcement: (a) effect of tensile stiffness; (b) effect of geosynthetic type; (c) effect of geosynthetic rigidity; and (d) effect of fill type.

Effect on the Relative Displacement between Soil and Reinforcement

The relative displacement, δ_{sg}, between soil and reinforcement is the difference between the reinforcement displacement (reinforcement displacement of the active reinforcement, u, in this paper) and the horizontal displacement of the soil adjacent to the reinforcement (soil displacement, x, at elevation $Y = 0$ in this paper; i.e., x_{sg}). The relative displacement is usually considered in literature as equivalent to the reinforcement displacement due to the difficulty of measuring reliable soil displacements. Fig. 9 shows the magnitude of δ_{sg} between soil and reinforcement at 80 mm from the front of the active reinforcement (i.e., $X = 305$ mm). Specifically, Figs. 9(a–d) show comparisons of the magnitudes of δ_{sg} between soil and reinforcement for test pairs to evaluate the effect of axial tensile stiffness, geosynthetic type, geosynthetic rigidity, and fill type, respectively. Here, δ_{sg} was obtained by subtracting the soil displacement measured by the artificial gravel particle adjacent to the reinforcement x4 (Fig. 3) from the reinforcement displacement at this location by interpolation between u1 and u2 [Fig. 2(a)].

Fig. 9(a) shows δ_{sg} between soil and reinforcement versus frontal tensile load for the tests conducted with W1-GT and W2-GT reinforcements using gravel as fill material. The results indicate that the δ_{sg} at the W1-GT interface was similar to that at the W2-GT interface up to δ_{sg} of 8 mm. However, beyond δ_{sg} of 8 mm, a significant difference was observed due to the difference in soil–reinforcement interaction (represented by C_i) between the two reinforcements, which developed primarily from the passive resistance in the W1-GT fabric, as previously discussed.

Fig. 9(b) shows δ_{sg} between soil and reinforcement versus frontal tensile load for the tests conducted with W1-GT and KN-GG reinforcements with gravel. The results indicate that δ_{sg} at the W1-GT interface was higher than that at the KN-GG interface due to the difference in soil–reinforcement interaction (represented by C_i) between the two reinforcements, as discussed previously. This implies that geogrids have a higher ability to interact with adjacent soil than geotextiles of the same tensile stiffnesses.

Fig. 9(c) shows δ_{sg} between soil and reinforcement versus frontal tensile load for the tests conducted with EX-GG and KN-GG reinforcements with gravel. The results indicate that δ_{sg} at the EX-GG interface was higher than that at the KN-GG interface due to the difference in soil–reinforcement interaction between the two reinforcements. Fig. 9(d) shows δ_{sg} between soil and reinforcement versus frontal tensile load for the tests conducted with gravel and sand with W1-GT reinforcements. The results indicate that δ_{sg} at the reinforcement interface was higher for the gravel as compared with the sand. This difference was due to the difference in soil–reinforcement interaction (represented by C_i) between the two fill materials with the reinforcement.

Overall, as with the case of soil to reinforcement displacement ratio, x_{sg}/u, discussed in the previous section, δ_{sg} increases with increasing soil–reinforcement interaction (represented by C_i), which controls the deformation of the soil mass adjacent to a loaded reinforcement layer. The relationship between δ_{sg} and C_i can be derived for the tests presented in this study as follows:

$$\delta_{sg} = \left(1 - \frac{C_i}{0.17}\right) u \tag{3}$$

Effect on the Interaction between Neighboring Reinforcement Layers

Fig. 10 shows the displacement profiles for the three reinforcement layers at active reinforcement frontal displacements, u1, of 5, 10, 15, and 20 mm in the test conducted with W1-GT reinforcement and gravel fill. Specifically, Figs. 10(a–e) shows the displacement profiles for the five tests conducted in this study: W1-GT-gravel. W2-GT-gravel, KN-GG-gravel, EX-GG-gravel, and W1-GT-sand combinations of reinforcements and soils, respectively. Displacements were plotted based on the same u1 rather than the same frontal tensile load for the following reasons: (1) being a better representation to the various tensile loading stages in the soil–reinforcement interaction tests; and (2) allowing a comparison in the shape of the displacement profile for reinforcements of various reinforcement stiffnesses and reinforcement resistance to tension.

The reinforcement displacement profiles show the magnitude of displacement along the lengths of the reinforcement layers as the active reinforcement is pulled (tensioned) from the reinforced soil mass. The load transfer was observed to reach the neighboring reinforcement layers, causing differential displacements (i.e., tensile strains). Additionally, the magnitudes of differential displacements were observed to increase as the tensile load in the active reinforcement increased and as load propagated along its embedment length, generating shear stresses along the soil–reinforcement interface. The comparisons among displacement profiles presented in Fig. 10 are discussed in detail next.

Before providing further discussion on each of the four comparisons considered in this study, Fig. 11 shows the average displacement (integrated area under the displacement profile divided by the reinforcement length) measured in the passive reinforcements (v_{av} and w_{av} for upper and lower reinforcement layers, respectively) versus the average displacement measured in the active reinforcement, u_{av}. It should be stressed that u_{av} is different than the frontal displacement, u1.

The results in Fig. 11 can be used to assess the load transfer from the active reinforcement to the passive reinforcements occurred at the same average active reinforcement displacement, u_{av}. That is, a comparison was made regarding the increasing soil–reinforcement interface shear displacement equivalent among tests conducted with different reinforcement types. This comparison provides insight into the difference between the various reinforcement types in relation to their ability to interact with neighboring reinforcement layers for a given soil medium and normal stress level. As shown in Fig. 11, the relationship between the displacements of the passive reinforcements was observed to be linear with the displacements of the active reinforcement in early loading stages. This relationship subsequently became nonlinear as the load-displacement relationship of the active reinforcement curved. The slope of the relationship indicates the extent of interaction among neighboring reinforcements. As the slope of the relationship increases, the interaction between the neighboring reinforcements increases.

A comparison of the reinforcement displacement profiles in Figs. 10(a and b) indicates that the displacement profiles of both reinforcement types, W1-GT and W2-GT, were very similar up to a frontal displacement of 20 mm. However, the measured displacements of the passive reinforcements were higher for W1-GT than for W2-GT. This is because W2-GT has a lower C_i than W1-GT and is likely to mobilize soil–reinforcement interface shear strength smaller than that of W1-GT for frontal displacements beyond 10 mm. The results in Fig. 11 indicate that W1-GT had a larger slope of the average passive and active displacements relationship as compared with W2-GT. The reduction in slope as loading (represented by average active reinforcement displacement) is increased, resulting in decreased interaction with the neighboring reinforcement layers, was lower for W1-GT as compared with that for W2-GT.

A comparison of the reinforcement displacement profiles in Figs. 10(a and c) shows higher displacements along the length of the active reinforcement for the profiles of W1-GT as compared with those of KN-GG. This difference increased as tensile loading progressed. In contrast, the profiles of the passive reinforcements showed lower displacement values for the W1-GT geotextile as compared with those measured for KN-GG. These results indicate higher reinforcement interaction with the neighboring layers for KN-GG as compared with W1-GT. This can be attributed to a higher soil–reinforcement interaction (represented by C_i) of KN-GG, which resulted in a greater load-transfer ability and a larger zone of influence. Moreover, despite having a smaller reinforcement displacement in the active reinforcement, KN-GG exhibited higher C_i than W1-GT, which had a larger reinforcement displacement.

For a better comparison of reinforcement displacement profiles, passive reinforcement profiles could be compared for conditions corresponding to the same magnitude of shear stresses (before shear stress peak is reached at any point along the reinforcement, i.e., quasi-elastic zone) generated along the active reinforcement. The results in Fig. 11 indicate that W1-GT had a larger slope for the relationship between the average displacements in passive reinforcements and active reinforcement (i.e., higher interaction between the neighboring reinforcements). The reduction in the slope as loading progressed, resulting in decreased interaction with the neighboring reinforcements, observed in the test conducted with W1-GT was larger as compared with the case of KN-GG.

A comparison of the reinforcement displacement profiles in Figs. 10(c and d) displays a slightly lower displacement along the reinforcement length for the profiles of EX-GG as compared with those of KN-GG. This was observed for both active and passive reinforcements. A comparison of the behavior in the early loading stages, up to failure of EX-GG, was conducted. As stated previously, for a better comparison of reinforcement displacement profiles, passive reinforcement profiles should be compared for the same amount of shear stresses generated along the active reinforcement. The results in Fig. 11 indicate that the interaction KN-GG had with its neighboring reinforcements was greater than that with EX-GG. However, interaction was observed for both reinforcements. This observation is a result of the greater elongation of EX-GG as compared with KN-GG. In short, this comparison revealed that EX-GG had slightly lower slope of the average passive and active displacements relationship, which resulted in slightly less interaction with neighboring reinforcements, as compared with that of KN-GG.

A comparison of the reinforcement displacement profiles in Figs. 10(a and e) indicates that the displacements measured for the active reinforcement for the test conducted with sand were lower than those measured for the test conducted with gravel. Conversely, the profiles of the passive reinforcements exhibit higher displacement values for the test conducted with sand than with gravel. The difference tends to become negligible and reverse at high tensile loads, which can be explained by the displacement profile of the active reinforcement. The reinforcement embedment in gravel mobilized more soil to transfer load for the same frontal displacement value. That is, a comparison between the displacement profiles of passive reinforcements tested at different normal stresses cannot gauge the effect of normal stress magnitude on the interaction among neighboring reinforcements. Yet, the results in Fig. 11 indicate that the sand can provide slightly larger interaction among neighboring reinforcements, which is represented by the slope of the relationship between the average passive and active

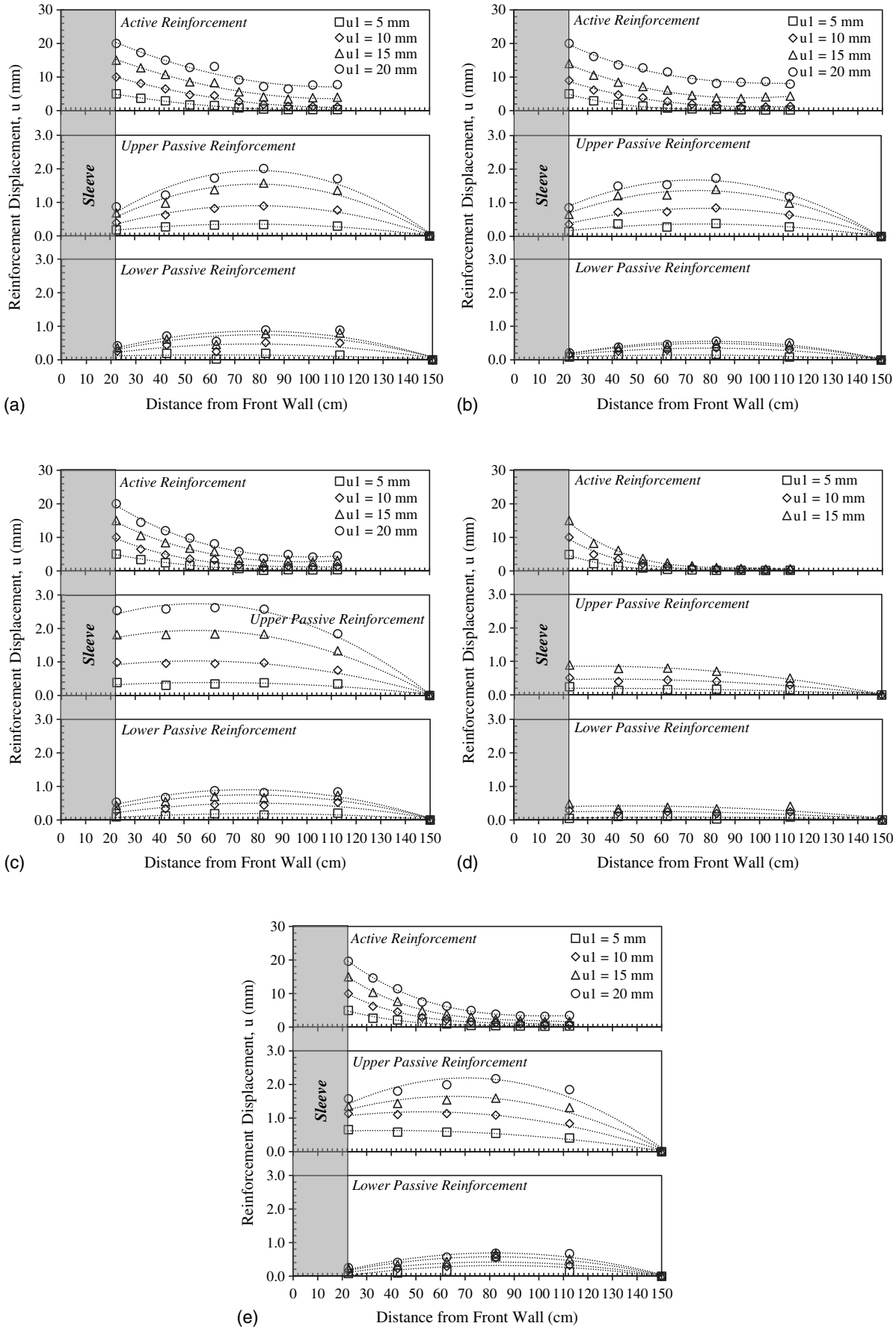

Fig. 10. Reinforcement displacement profiles at various frontal displacements u1: (a) W1-GT-gravel; (b) W2-GT-gravel; (c) KN-GG-gravel; (d) EX-GG-gravel; and (e) W1-GT-sand.

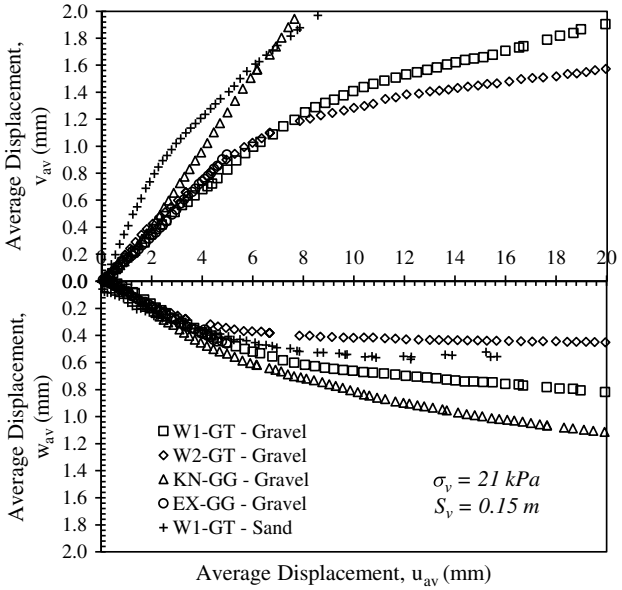

Fig. 11. Average displacements in passive reinforcements, v_{av} and w_{av}, relative to average displacement in active reinforcement, u_{av}.

reinforcement displacements. Although an opposite trend was observed in the comparison between the average displacements of the lower passive reinforcement, the evaluation of the other parameters in this study supports the indication that neighboring reinforcements have higher ability to interact in sand than in gravel.

Overall, the interpretation of the results generated from the tests conducted in this study suggests that the interaction among neighboring reinforcements (represented by v_{av}/u_{av} and w_{av}/u_{av}) increases with increasing soil–reinforcement interaction (represented by C_i).

Conclusions

A comprehensive testing program was conducted adopting the experimental approach and equipment developed by Morsy (2017). The testing program was tailored to evaluate the effects of reinforcement and soil types (i.e., soil–reinforcement interface combinations) on soil–reinforcement interaction as well as the interaction between neighboring reinforcements. This investigation yielded the following findings:

- The higher the soil–reinforcement interaction (represented in this study by C_i), the higher the ability of the reinforcement to transfer load to the soil and neighboring reinforcement layers for a given soil medium and normal stress level.
- In light of the frontal tensile load-displacement curve evaluation, the results presented in this study indicated that geotextile reinforcements with ability to soil particle intrusion, due to lower fabric integrity, are capable of developing passive resistance, which enhances the soil–reinforcement interaction (i.e., provides higher C_i). Geogrid reinforcements are more capable of interacting with soils than geotextiles. The contribution of passive resistance to soil–reinforcement interaction likely outweighs the contribution of interface friction. That is, geogrid reinforcements are likely to form stronger composite reinforced soil masses than geotextile reinforcements. Flexible (knitted) geogrids have higher ability to interact with soil particles than rigid (extruded) geogrids. Sand fills can provide a larger number of contacts (interlocking points) with a geotextile per unit area than gravel fills of similar friction angles.
- In light of the horizontal soil displacement evaluation, the results presented in this study indicated that the soil adjacent to active reinforcements exhibited higher displacement gradients than the soil farther away from reinforcements because of yielding in the internal shear strength of the fill material as internal shear strain increases, which impedes the load transfer from the reinforcement to distance farther away from the reinforcement. In short, the composite behavior of the reinforced soil mass tends to diminish at large strain levels.
- The relationship between the horizontal soil displacements adjacent to the reinforcement and the reinforcement displacements is practically linear. The slope of the linear relationship (i.e., soil to reinforcement displacement ratio) was found to increase proportionally with increasing C_i. The slope of the linear relationship between C_i and the soil to reinforcement displacement ratio was found to be 0.17. Overall, it was concluded that the soil–reinforcement interaction (represented by C_i) controls the deformation of the soil mass adjacent to a loaded reinforcement. The synergy between the soil and reinforcements increases with increasing C_i.
- In light of the evaluation of the relative displacements between soils and reinforcements, the results presented in this study indicated that the relative displacement increases with increasing soil–reinforcement interaction (represented by C_i).

Data Availability Statement

All data, models, and code generated or used during the study appear in the published article.

Acknowledgments

The work presented in this paper was conducted while the first author pursued his doctoral degree at the University of Texas at Austin. This research was partly supported by the National Cooperative Highway Research Program (NCHRP) under Project 24-41. The opinions presented in this paper are exclusively those of the authors and not necessarily those of the NCHRP.

References

Alshibli, K. A., and S. Sture. 1999. "Sand shear band thickness measurements by digital imaging techniques." *J. Comput. Civ. Eng.* 2 (13): 103–109. https://doi.org/10.1061/(ASCE)0887-3801(1999)13:2(103).

Bareither, C., T. Edil, C. Benson, and D. Mickelson. 2008. "Geological and physical factors affecting the friction angle of compacted sands." *J. Geotech. Geoenviron. Eng.* 134 (10): 1476–1489. https://doi.org/10.1061/(ASCE)1090-0241(2008)134:10(1476).

Fannin, R. J., and D. M. Raju. 1993. "On the pullout resistance of geosynthetics." *Can. Geotech. J.* 30 (3): 409–417. https://doi.org/10.1139/t93-036.

Jacobs, F., M. Ziegler, and A. Ruiken. 2013. "Experimental investigation of the stress-strain behaviour of geogrid reinforced soil." In *Proc., GeoAfrica 2013*. Austin, TX: International Geosynthetics Society.

Ketchart, K., and J. T. H. Wu. 2002. "A modified soil-geosynthetic interactive performance test for evaluating deformation behavior of GRS structures." *ASTM Int.* 25 (4): 405–413. https://doi.org/10.1520/GTJ11294J.

Leshchinsky, D., V. Kaliakin, P. Bose, and J. Collin. 1994. "Failure mechanism in geogrid-reinforced segmental walls: Experimental implications." *Soils Found.* 34 (4): 33–41. https://doi.org/10.3208/sandf1972.34.4_33.

Leshchinsky, D., and C. Vulova. 2001. "Numerical investigation of the effects of geosynthetic spacing on failure mechanisms in MSE block walls." *Geosynthetics Int.* 8 (4): 343–365. https://doi.org/10.1680/gein.8.0199.

Morsy, A. M. 2017. "Evaluation of soil-reinforcement composite interaction in geosynthetic-reinforced soil structures." Ph.D. dissertation, Dept. of Civil, Architectural, and Environmental Engineering, Univ. of Texas at Austin.

Morsy, A. M., D. Leshchinsky, and J. G. Zornberg. 2017a. "Effect of reinforcement spacing on the behavior of geosynthetic-reinforced soil." In *Proc., Geotechnical Frontiers 2017*, 112–125. Reston, VA: ASCE.

Morsy, A. M., G. H. Roodi, and J. G. Zornberg. 2018. "Evaluation of soil-reinforcement interface shear band." In *Proc. 11th Int. Conf. on Geosynthetics (ICG), Paper No. S18-05*. Austin, TX: International Geosynthetics Society.

Morsy, A. M., J. G. Zornberg, B. R. Christopher, D. Leshchinsky, B. F. Tanyu, and J. Han. 2017b. "Experimental approach to characterize soil-reinforcement composite interaction." In *Proc., 19th Int. Conf. on Soil Mechanics and Geotechnical Engineering (ICSMGE)*, 451–454. London: International Society for Soil Mechanics and Geotechnical Engineering.

Morsy, A. M., J. G. Zornberg, J. Han, and D. Leshchinsky. 2019a. "A new generation of soil-geosynthetic interaction experimentation." *Geotext. Geomembr.* 47 (4): 459–476. https://doi.org/10.1016/j.geotexmem.2019.04.001.

Morsy, A. M., J. G. Zornberg, D. Leshchinsky, and J. Han. 2019b. "Soil-reinforcement interaction: Effect of reinforcement spacing and normal stress." *J. Geotech. Geoenviron. Eng.* 45 (12): 04019115. https://doi.org/10.1061/(ASCE)GT.1943-5606.0002180.

Nicks, J. E., M. T. Adams, P. S. K. Ooi, and T. Stabile. 2013. *Geosynthetic reinforced soil performance testing—Axial load deformation relationships*. Rep. No. FHWA-HRT-13-066. McLean, VA: Federal Highway Administration.

Ruiken, A., M. Ziegler, L. Vollmert, and S. Höhny. 2011. "Investigation of the compound behavior of geogrid reinforced soil." In *Proc. 15th European Conf. on Soil Mechanics and Geotechnical Engineering (ECSMGE)*. London: International Society for Soil Mechanics and Geotechnical Engineering.

Shen, P., J. Han, J. G. Zornberg, A. M. Morsy, D. Leshchinsky, B. F. Tanyu, and C. Xu. 2019. "Two and three-dimensional numerical analyses of geosynthetic-reinforced soil (GRS) piers." *Geotext. Geomembr.* 47 (3): 352–368. https://doi.org/10.1016/j.geotexmem.2019.01.010.

Ziegler, M. 2011. "Interaction of soil reinforcement as key issue for ground reinforcement." In *Proc., 15th European Conf. on Soil Mechanics and Geotechnical Engineering (ECSMGE)*. London: International Society for Soil Mechanics and Geotechnical Engineering.

Zornberg, J. G. 2002. "Peak versus residual shear strength in geosynthetic-reinforced soil design." *Geosynthetics Int.* 9 (4): 301–318. https://doi.org/10.1680/gein.9.0220.

Zornberg, J. G., A. M. Morsy, B. M. Kouchaki, B. R. Christopher, D. Leshchinsky, J. Han, B. F. Tanyu, F. T. Gebremariam, P. Shen, and Y. Jiang. 2018. *Defining the boundary conditions for composite behavior of geosynthetic reinforced soil (GRS) structures*. Project NCHRP 24-41. Washington, DC: Transportation Research Board.

Zornberg, J. G., A. M. Morsy, B. M. Kouchaki, B. R. Christopher, D. Leshchinsky, J. Han, B. F. Tanyu, F. T. Gebremariam, P. Shen, and Y. Jiang. 2019. *Proposed refinements to design procedures for geosynthetic reinforced soil (GRS) structures in AASHTO LRFD bridge design specifications*. NCHRP Web Document 260. Washington, DC: Transportation Research Board.